AIP Journal of Applied Physics

Dielectric and ferroelectric response of compositionally graded bilayer and trilayer composites of BaTiO 3 and 0.975 BaTiO 3 – 0.025 Ba (Cu 1 / 3 Nb 2 / 3) O 3

Deepam Maurya, Natthapong Wongdamnern, Rattikorn Yimnirun, and Shashank Priya

Citation: Journal of Applied Physics **108**, 124111 (2010); doi: 10.1063/1.3514125
View online: http://dx.doi.org/10.1063/1.3514125
View Table of Contents: http://scitation.aip.org/content/aip/journal/jap/108/12?ver=pdfcov
Published by the AIP Publishing

Dielectric and ferroelectric response of compositionally graded bilayer and trilayer composites of $BaTiO_3$ and $0.975BaTiO_3-0.025Ba(Cu_{1/3}Nb_{2/3})O_3$

Deepam Maurya,[1] Natthapong Wongdamnern,[2] Rattikorn Yimnirun,[3] and Shashank Priya[1,a)]

[1]*CEHMS, Department of Materials Science and Engineering, Virginia Tech, Virginia 24061, USA*
[2]*Department of Physics and Materials Science, Chiang Mai University, Chiang Mai 50200, Thailand*
[3]*School of Physics, Institute of Science, Suranaree University of Technology, Nakhon Ratchasima 30000, Thailand*

(Received 11 August 2010; accepted 9 October 2010; published online 29 December 2010)

In this paper, we report the dielectric and ferroelectric response of compositionally graded bilayer and trilayer composites consisting of $BaTiO_3$ (BT) and $0.975BaTiO_3-0.025Ba(Cu_{1/3}Nb_{2/3})O_3$ (BTBCN). Two types of graded bilayer samples were synthesized, one with same thickness of BT and BTBCN while other with different layer thicknesses. The graded trilayer sample consisted of BT layer sandwiched between two BTBCN layers of equal thickness. Scanning electron microscopy and transmission electron microscopy images showed a sharp interface with needle-shape domains across the interface. The domain size on BT side was found to be larger than that on BTBCN side. The temperature dependence of dielectric response for all composite systems was found to exhibit shifting in characteristic Curie peak compared to constituent material which was associated to coupling between layers. Moreover, the differences in grain size, tetragonality, domain mobility of each layer was found to perturb the electrical response of composite. The polarization mismatch between uncoupled BT and BTBCN established internal electric field in composite specimen and defined new polarization states in each layer by perturbing free energy functional of the composite specimen. Dynamic hysteresis behaviors and power-law scaling relations of all specimens were determined from polarization-electric field hysteresis loop measurements as a function of frequency. All systems were found to exhibit similar dynamic scaling relationships. Hysteresis area $\langle A \rangle$, P_r, and E_C decreased with increasing frequency due to delayed response but increased with increasing applied electric field due to enhancement of driving force. Trilayer system was found to exhibit strong internal-bias field and double hysteresis behavior. The coupling effect resulting due to polarization mismatch between layers had substantial influence on the dynamic hysteresis behavior and power-law scaling relations. © *2010 American Institute of Physics*. [doi:10.1063/1.3514125]

I. INTRODUCTION

Ferroelectric random access memory has been gaining interest as it can provide nonvolatile memory operation with fast writing time while reducing the power requirement.[1] Ferroelectric materials are also being used as gate in ferroelectric memory field-effect transistor (FeMFET) (Refs. 2–4) providing a nondestructive readout operation with high density. The stored dipole moments in the ferroelectric material can adjust the threshold voltage of a FeMFET, and thus drain current of each switching state can be discriminated and identified as a logic state in memory.[1] In these applications, the switching capability and energy loss during the operation of ferroelectric gate is quite important. Both of these parameters are dependent upon the hysteresis behavior of ferroelectric material. Ideally, one would like to achieve a slim hysteresis loop with large remanence and low coercivity.

In order to develop ferroelectric materials with adequate hysteresis behavior as required for new generation of memories, efforts have been made on developing graded structures in the form of bilayer, trilayer, and multilayers.[5–7] Such structures offer the possibility of tuning the hysteresis loops by modulating the parameters such as leakage current, sharpness of the interface and ferroelectric–antiferroelectric exchange coupling. However, most of the work in this area has been limited to thin films where besides material parameters and interface phenomenon, additional factors such as clamping from the substrate, residual stress due to difference in thermal expansion, and epitaxy influences the overall hysteresis behavior. We decided to investigate the bulk graded ferroelectrics for two specific reasons: (i) to better understand the physics governing the dynamic hysteresis behavior and (ii) to deterministically model the hysteretic scaling relationships. The prediction of hysteresis behavior with applied electric field amplitude and frequency can be accomplished by constructing the dynamic hysteresis and scaling rules.[8–10] Dynamic hysteresis model provides the changes in hysteresis area $\langle A \rangle$, coercive field (E_c), and remnant polarization (P_r) as function of amplitude of applied field (E_o) and frequency (f).[11] We synthesized bilayer and trilayer ferroelectric graded structures with following variations: (i) single layer thick film of pure $BaTiO_3$ (BT) with thickness of 1 mm, (ii) bilayer structure with equal layer thickness of 0.5 mm for BT and $0.975BaTiO_3-0.025Ba(Cu_{1/3}Nb_{2/3})O_3$ (BTBCN), (iii) bilayer structure with unequal thickness of 0.650 mm for BT

a)Electronic mail: spriya@mse.vt.edu.

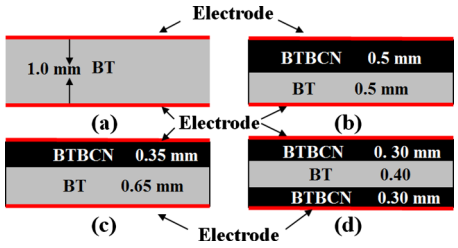

FIG. 1. (Color online) Schematic representation of the bilayer and trilayer thick films (a) BT, (b) bilayer with equal thickness of BT and BTBCN layer (0.5 mm each), (c) bilayer with higher thickness of BT (0.65 mm) and BTBCN (0.35 mm), and (d) trilayer with 0.3 mm thickness of each BTBCN layer and 0.4 mm BT layer sandwiched in between them.

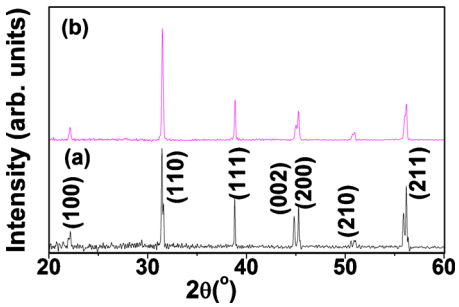

FIG. 2. (Color online) XRD patterns recorded at RT on (a) BT and (b) BTBCN side of the bilayer.

and 0.350 mm for BTBCN, and (iv) trilayer structure with 0.40 mm layer of BT sandwiched between two layers of BTBCN with thickness of 0.30 mm. All these structures are schematically shown in Fig. 1. It was observed that coupling resulting due to polarization mismatch between layers changes the free energy function and influences the dynamic hysteresis behavior and power-law scaling relations.

II. EXPERIMENTAL

BT and BTBCN were synthesized by using mixed oxide route. Calcined powders were mixed with binder system and used for tape casting. Dried tapes of thickness 60 μm were cut to desired dimensions and laminated to fabricate bilayer and trilayer structures. Laminated stacks were sintered at 1350 °C for 2h. Phase evolution for all specimens was determined by using Philips Xpert Pro XRD system (Almelo, the Netherlands). Dielectric constant and tangent loss factor was determined as a function of temperature at selected frequencies using HP 4284A LCR meter connected to a computer-controlled high temperature furnace. The surface microstructure of sintered samples was observed using Zeiss Leo scanning electron microscope (SEM). Transmission electron microscopy (TEM) was performed by using FEI Titan 300 on specimen prepared by using focused ion beam (FEI Helios 600 NanoLab). Polarization-electric field (P-E) hysteresis measurements were conducted by using modified Sawyer–Tower bridge Precision II (Radiant Technologies). All the measurements were repeated on at least three samples to confirm the repeatability.

III. RESULTS AND DISCUSSION

A. Domain and interface structure

Figure 2 shows the room temperature (RT) x-ray diffraction (XRD) patterns for bilayer specimen from both BT and BTBCN sides. It can be seen that both the layers crystallized in perovskite phase with tetragonal symmetry. However, the splitting of (200) peak was prominent in the XRD pattern recorded on BT side. The tetragonality (c/a) calculated using (200) and (002) peaks was found to be 1.01 and 1.006 for BT and BTBCN side, respectively. The decrease in tetragonality was generally coupled with lowering of transition temperature and decrease in grain size,[12] which is consistent with SEM micrographs and $\varepsilon(T)$ plots explained later. This difference in tetragonality between BT and BTBCN defines difference in principle strain S_s, given as $S_s=(c/a-1)$. The magnitude of S_s was found to be 0.01 for BT and 0.006 for BTBCN resulting in strain gradient across the interface between the two coupled layers in bilayer.

Figures 3(a)–3(c) show the SEM micrograph of interface at various magnifications. There is clear difference in the average grain size across the interface (shown by solid line), where grains on BT side were found to be much larger ~32 μm than that on BTBCN side ~0.64 μm (computed using line-intercept method). The magnified view of interface region in Fig. 3(c) depicts a sharp interface indicating that there was limited diffusion of Cu and Nb across the interface. EDS (energy dispersive x-ray spectroscopy) detector in SEM analysis was not able to find any trace of Cu and Nb across the interface. Using Fig. 3(d), the effective thickness of interface can be estimated to be ~75 nm in case of bilayer, and ~150 nm in the case of trilayer with two interfaces. Figure 3(d) shows the TEM image of specimen across the interface. Selected area electron diffraction (SAED) pattern of corresponding sides are shown in inset of Fig. 3(d). In these SAED patterns, the zone axis of BT side was [111] and that of BTBCN side was [110]. Needle shaped domain structure was found to be formed on both BT and BTBCN side, however domains on BT side had larger width than that on BTBCN side. This is quite interesting observation and provides us the key to modify the polarization response. The

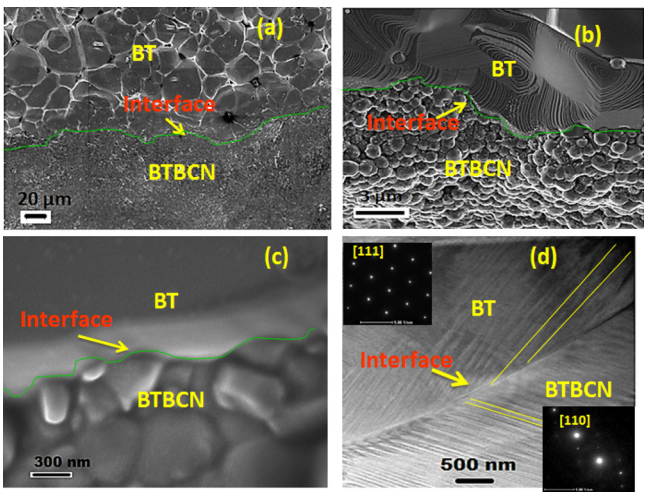

FIG. 3. (Color online) [(a)–(c)] SEM micrographs of the interface at various magnifications, (d) TEM image of the domain structure across the interface (inset showing SAED pattern).

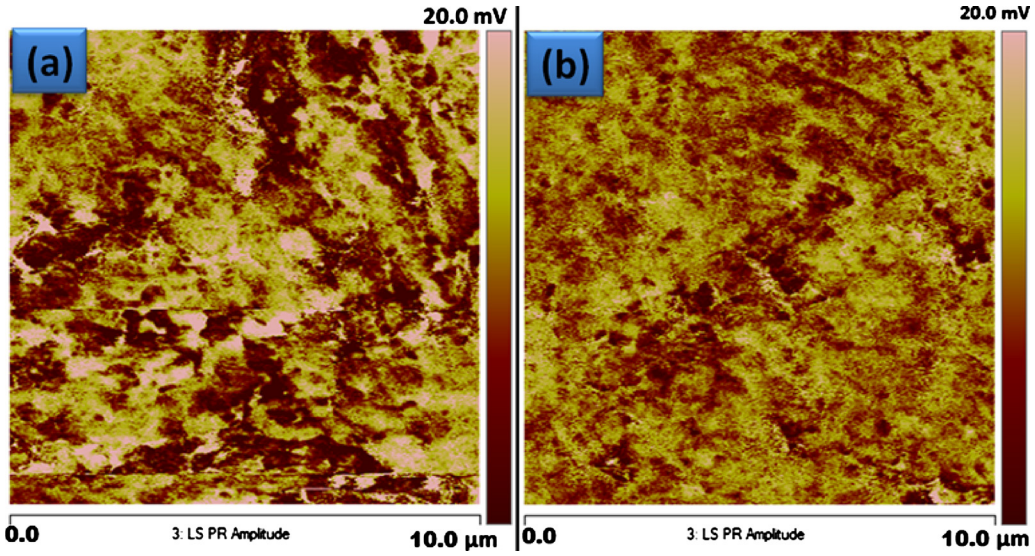

FIG. 4. (Color online) PFM image of (a) BT side and (b) BTBCN side.

difference in grain size (as observed in SEM images) results in the variation in domain size and width, which in turn influences the polarization. In randomly oriented polycrystalline ceramics, the domain size (D) is related to grain size (G) as:[13]

$$D \propto G^p, \tag{1}$$

where

$$p < 1/2 \quad \text{for} \quad G > 10 \ \mu\text{m},$$

$$p = 1/2 \quad \text{for} \quad 10 \ \mu\text{m} > G > 1 \ \mu\text{m},$$

$$p > 1/2 \quad \text{for} \quad G < 1 \ \mu\text{m}.$$

Using Eq. (1), we can approximate the domain size of BT material by taking $p=1/3$ (typical value) in the case of grain size >10 μm.[13] Substituting the value of grain size calculated from SEM micrographs in Eq. (1) and rewriting the above equation to find the exponent p for BTBCN material as:

$$D_{\text{BT}}/D_{\text{BTBCN}} = (32)^{1/3}/(0.64)^p. \tag{2}$$

The domain size obtained from TEM analysis was used to determine the ratio in Eq. (2), which was roughly found to be 4. Thus, the exponent p for BTBCN material with grain size of 0.64 μm was calculated to be 0.52. This difference in the domain exponent results in the varying polarization across the interface. Combined with strain–gradient, this result indicates the formation of graded structure.

Figures 4(a) and 4(b) show the piezoresponse force microscopy (PFM) images of BT and BTBCN side, respectively, where the variation in contrast indicates regions with different piezoelectricity. If the sample was single domain structure than the image produced would be all of same color. Comparing the two images, it can be seen that there is difference in the magnitude of the piezoelectric response, with BTBCN exhibiting higher piezoelectric response than that of BT. Using Berlincourt d_{33} meter, the piezoelectric coefficient of individual layers of BT and BTBCN was found to be 144 and 330 pC/N. These measurements were in agreement with the PFM information showing higher piezoelectric activity for the BTBCN phase.

Figures 5(a)–5(e) shows the variation in dielectric constant (ε) and tangent loss factor (tan δ) as a function of temperature (T) at different frequencies for various specimens. It is known that BT and BTBCN have Curie temperature (T_c) of 125 °C and 80 °C, respectively.[14] The characteristic transition peaks of BT and BTBCN can be marked in the $\varepsilon(T)$ plots as shown in Figs. 5(a) and 5(b). The transition temperatures of BT and BTBCN can be found in the graded bilayer and trilayer specimens with minor shifts. The Curie temperature of BT was shifted toward lower temperature (~117 °C) while that of BTBCN was shifted toward higher temperature (~90 °C), which can be attributed to strain gradient present across the interface. The magnitude of maxima in dielectric constant, $\varepsilon(T_m)$, was found to decrease for the composite specimens. In the case of graded trilayer, the peak in the dielectric curve due to BTBCN was more obvious due to higher effective thickness of two BTBCN layers. These results clearly show that there was influence of interface on the overall system properties and dielectric response of the composite was a combination of individual components. Further these results combined with the gradient in domain size and widths confirm the formation of graded structure. More information on grading and interface coupling could be obtained by invoking phenomenology.

For an uncoupled and unconstrained tetragonal BT, the free energy in terms of polarization can be expressed as:[15]

$$G_1(P,T) = G_{o1}(T) + 1/2a_1P_1^2 + 1/4a_2P_1^4 + 1/6a_3P_1^6, \tag{3}$$

where $G_o(T)$ is the energy in paraelectric state. For the isothermal case, the electric field acting on the ferroelectric material, expressed in terms of P_1, can be obtained as:

$$E_1 = dG_1/dP_1 = a_1P_1 + a_2P_1^3 + a_3P_1^5. \tag{4}$$

Similarly for BTBCN the electric field is given as:

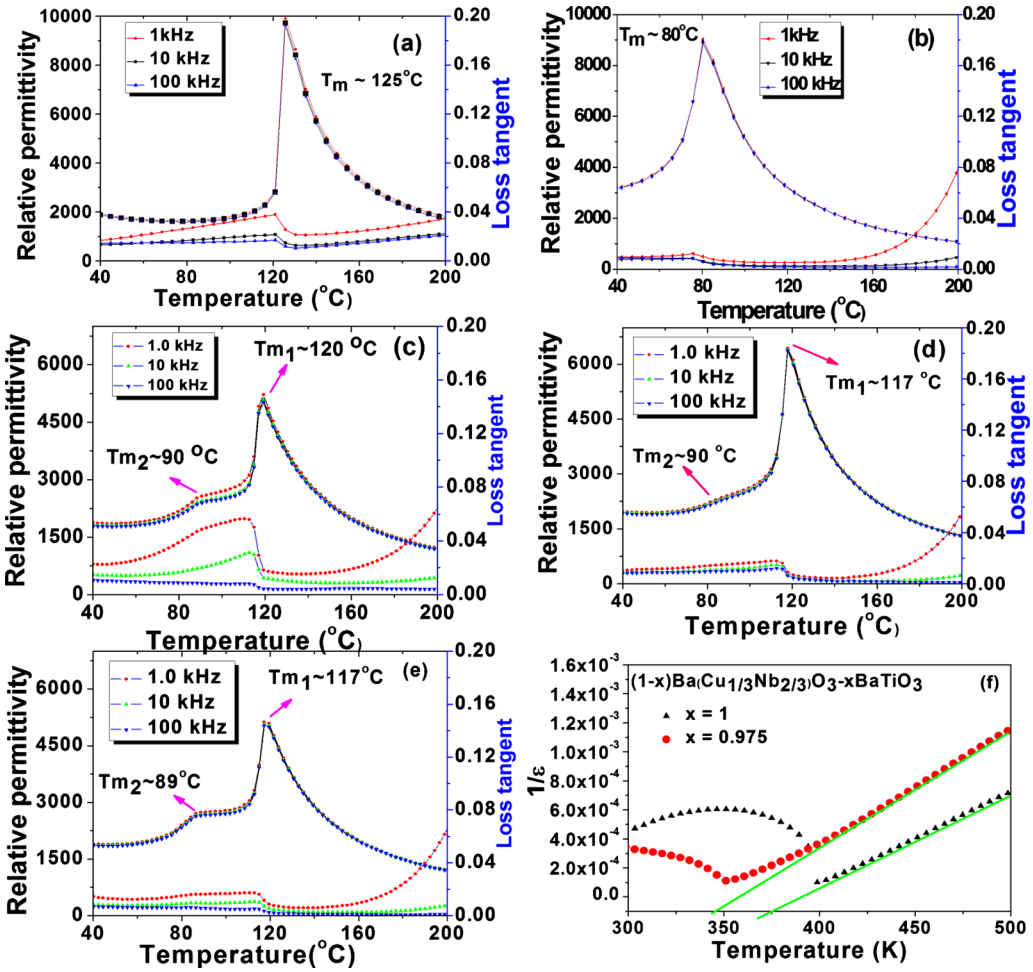

FIG. 5. (Color online) Temperature dependence of relative permittivity for (a) BT, (b) BTBCN, (c) bilayer with equal thickness, (d) bilayer with unequal thickness, (e) trilayer with BT layer sandwiched between two BTBCN layers, and (f) $1/\varepsilon$ vs temperature plot.

$$E_2 = dG_2/dP_2 = b_1P_2 + b_2P_2^3 + b_3P_2^5, \tag{5}$$

where G_1 and G_2 are free energy of layer 1 and 2 in its high-temperature PE state, P_1 and P_2 are the polarizations of layers 1 and 2 and a_1, a_2, a_3, b_1, b_2, b_3 are the Landau coefficients. The coefficients a_1 and b_1 have temperature dependence given by the Curie–Weiss law as $a_1=(T_o - Tc_1)/\varepsilon_o C_1$ and $b_1=(T_o-Tc_2)/\varepsilon_o C_2$, where ε_o is the permittivity of free space, Tc_1, Tc_2 and C_1, C_2 are the Curie–Weiss temperature and constant of uncoupled layer 1 and 2. The other coefficients in free energy function are assumed to be temperature independent. By equating Eqs. (4) and (5) to zero, spontaneous polarization (P) corresponding to two polarization states of each layer can be obtained. Figure 5(f) was used to compute the magnitude of $(T_o-Tc_1)\sim -24.15$ K for BT layer and $(T_o-Tc_2)\sim -5.88$ K for BTBCN layer. The values of Curie constant calculated from experimental data were found to be $\sim 1.6\times 10^5$ K for BT and $\sim 1.4\times 10^5$ K for BTBCN.

After coupling of both layers in graded bilayer and trilayer structure, the free energy (G) and electric field (dG/dP) values would be different as observed in terms of differences in $\varepsilon(T)$ plots. Suppose $E_{i,1}$ and $E_{i,2}$ are the internal electric fields in BT and BTBCN layers given as:[16,17]

$$E_{i1} = -1/\varepsilon_0(P_1 - \langle P\rangle) = \alpha/\varepsilon_0(P_2 - P_1), \tag{6}$$

and

$$E_{i2} = -1/\varepsilon_0(P_2 - \langle P\rangle) = (1-\alpha)/\varepsilon_0(P_1 - P_2), \tag{7}$$

where P_1 and P_2 are new polarization states in layer 1 and layer 2 respectively after coupling, $\langle P\rangle=(1-\alpha)P_1+\alpha P_2$ is the average polarization and α is the relative volume fraction. The total free energy function incorporating the potential energies of internal fields E_1 and E_2 is given by:[16]

$$G_\Sigma = (1-\alpha)[G_1(P_1) - EP_1 - 1/2\xi E_{i1}P_1] + \alpha[G_2(P_2) - EP_2 - 1/2E_{i2}P_2] + G_S/h + G_{el} - JP_1P_2, \tag{8}$$

where G_{el} is the elastic energy of the polarization-free misfit. The energy of interface G_S/h can be neglected due to very small correlation length of ferroelectric[18] in comparison to the total thickness of bilayer (~ 1000 μm). The last term in above equation is interlayer (interfacial) coupling and J is the coupling coefficient (interfacial exchange interaction coefficient) given as:[16]

$$J = \alpha(1-\alpha)\xi/\varepsilon_0. \tag{9}$$

Above relation demonstrates that the coupling between layers can be controlled by either the volume fraction of each

TABLE I. Magnitude of polarization in quasistatic frequency (0.1 Hz) regime.

Systems	P_r in subcoercive field (E_{c-}) regime (1 kV/cm) ($\mu c/cm^2$)	P_{max} in saturated field (E_{c+}) regime ($\mu c/cm^2$)	Polarization ratio=$P_r(E_{c-})/P_{max}(E_{c+})$
BTBCN single layer	0.15	19.2	0.007 81
BT single layer	0.11	16.8	0.006 55
Bilayer with equal thickness	0.14	16.5	0.008 48
Bilayer with unequal thickness	0.07	15.2	0.004 61
Trilayer	0.07	12.1	0.005 79

layer or by modifying the free carrier content quantified by coefficient ξ. "ξ" is measure of the free charge density with respect to the bound charge at the interlayer interface given as $\xi=1-\rho_f/\rho_b, \rho_b$ is the bound charge density and ρ_f is the free charge density. The two limiting values, $\xi=1$ and $\xi=0$ correspond to perfect insulating and semiconducting ferroelectric bilayers. Assuming polarization $\vec{P}$ varies from point to point within the interfacial region, the resulting bound charge density can be written as:

$$\rho_b = -\vec{\nabla} \cdot \vec{P}. \tag{10}$$

Using differential form of Gauss's law, the divergence of electric field is given as:

$$\vec{\nabla} \cdot \vec{E} = \frac{\rho}{\varepsilon_o} = \frac{\rho_b + \rho_f}{\varepsilon_o}. \tag{11}$$

Combining Eqs. (10) and (11), we can derive the relation for free charge density as:

$$\vec{\nabla} \cdot \varepsilon_o \vec{E} = -\vec{\nabla} \cdot \vec{P} + \rho_f,$$

or

$$\rho_f = \vec{\nabla} \cdot \varepsilon_o \vec{E} + \vec{\nabla} \cdot \vec{P} = \vec{\nabla} \cdot (\varepsilon_o \vec{E} + \vec{P}) = \vec{\nabla} \cdot \vec{D}, \tag{12}$$

where $\vec{D}=(\varepsilon_o \vec{E}+\vec{P})$ is the displacement vector. In quasistatic frequency regime (<1 Hz) and below subcoercive field, the contribution from free charge polarization is dominant. In saturated field and quasistatic frequency regime, alignment of domains contributes to resultant polarization, which provides estimation of bound charge density. Table I lists the values of polarization for subcoercive field (E_{c-} =1 kV/cm) and maximum polarization in saturated field (E_{c+}) regime for layered systems at 0.1 Hz. Taking the ratio of the polarization magnitudes in E_{c-} and E_{c+} regime, an indication for the changes in free and bound charge density can be obtained ($\sim \rho_f/\rho_b$). The polarization ratio shown in Table I indicates a significant drop for the graded bilayer with unequal thickness and trilayer structure which reflects the increase in coupling coefficient. This analysis neglects the contribution from interface which is not realistic but it does provide an explanation for the changes observed in hysteresis behavior as explained later. Further, this analysis confirms the observation on influence of graded structure on ferroelectric properties.

B. Ferroelectric hysteresis behavior

The hysteresis profiles with various frequencies (f) and electric fields (E_0) were obtained for BT single layer, BT-BTBCN graded bilayer with equal and unequal thicknesses, and BTBCN-BT-BTBCN graded trilayer ceramic systems. Examples of hysteresis profiles are shown in Figs. 6(a) and 6(b) for BT single layer system. Other systems, i.e., graded bilayer with equal and unequal thicknesses and trilayers, exhibited very similar behaviors. At fixed E_0, the hysteresis loop area $\langle A \rangle$, remnant polarization (P_r) and coercive field (E_C) decreased with an increase in frequency [Fig. 6(a)] because of the delayed response of domain switching and polarization reversal which diminishes hysteresis loop size.[19] At fixed f, remnant polarization (P_r) increases with an increase in E_0 [Fig. 6(b)] as larger E_0 provides higher level of driving force responsible for switching of ferroelectric domains. Higher driving force enhances the domain volume and consequently total polarization including hysteresis parameters.[11]

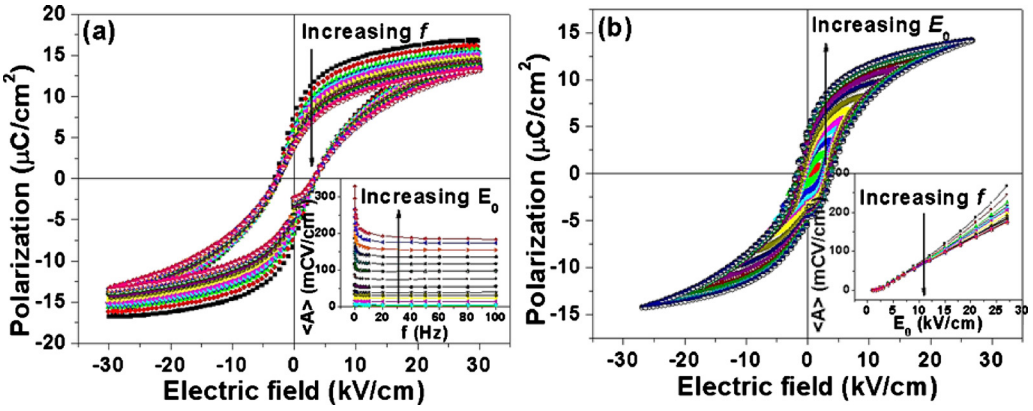

FIG. 6. (Color online) *P-E* hysteresis loops of BT single layer system (a) various f with fixed E_0=30 kV/cm, and (b) various E_0 with fixed f=10 Hz.

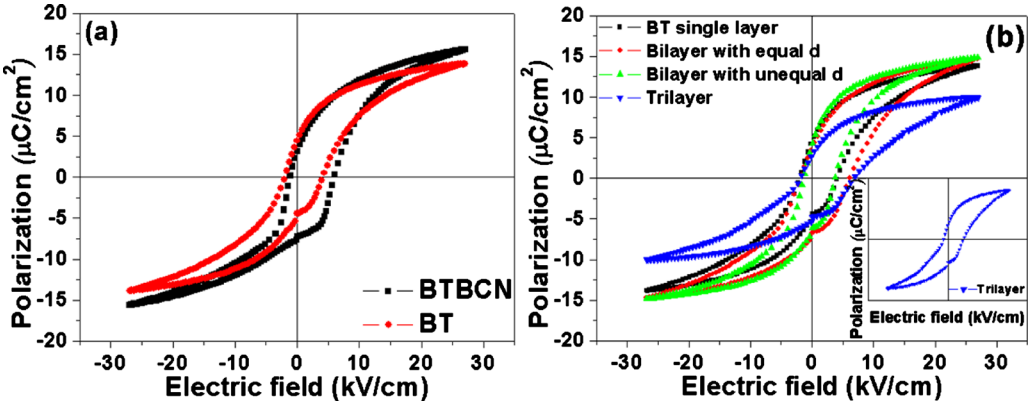

FIG. 7. (Color online) (a) *P-E* hysteresis loops of BTBCN and BT layers at fixed $f=50$ Hz and $E_0=27$ kV/cm, and (b) *P-E* hysteresis loops of multilayer systems with fixed $f=50$ Hz and $E_0=27$ kV/cm.

Figure 7(a) compares the *P-E* hysteresis loop of BTBCN with BT. Both these compositions are ferroelectric with tetragonal perovskite structure at RT (Ref. 20) and as seen in this figure, the polarization of BTBCN is higher than that of BT. Hysteresis loops of both materials were found to be shifted toward positive side on electric field axis implying the presence of internal-bias field mainly arising from electronic defects. The polarization switching mechanisms in BT single crystals have been attributed to nucleation of antiparallel domains and their growth by domain wall motion.[21–23] In polycrystalline ceramics, the polarization switching is strongly influenced by presence of grain boundaries, space charges, charged defects and surfaces.[24–29] Presence of charged defects will result in the formation of internal-bias field as commonly observed for the hard piezoelectric materials by pinning the domain boundaries. The coercive field broadness ($2E_C$) of BTBCN was larger than that of BT. The *P-E* hysteresis loops of BT single layer and BT-BTBCN layers formed as graded bilayer and trilayer ceramic systems are compared in Fig. 7(b). The polarization value of graded trilayer ceramic system was lowest as compared with rest of the cases but it possesses the largest coercive field (E_C). The coercive field (E_C) value on positive side was higher than that on negative side for all systems which is further indication of built-in internal-bias field.[30]

To quantify internal-bias field in each system, we can utilize following relations:[31]

$$E_1 = E_C + E_i, \tag{13}$$

$$E_2 = -E_C + E_i, \tag{14}$$

thus,

$$E_i = (E_1 + E_2)/2, \tag{15}$$

where E_1 and E_2 are electric field intercepts on positive and negative side respectively, E_C is the magnitude of coercive field with no internal-bias and E_i is the magnitude of internal-bias field. The effect of internal-bias field on the coercive field can be determined by expressing the rate of motion of domain boundaries as:

$$v = \mu E, \tag{16}$$

and

$$\mu = (3\delta)/2P_0\Gamma, \tag{17}$$

where μ is the mobility of domain wall, δ is its half-width, Γ is the viscosity of domain wall motion, and P_0 is the spontaneous polarization.[32] The switching time was characterized by the time of inter-growth of domain to the crystallite half-width $d/2$ given by the relation:

$$t = d/[2v(E_C)] = 1/f \tag{18}$$

Combing Eqs. (16)–(18), we can obtain:

$$E_C = (P_0\Gamma df)/\delta, \tag{19}$$

which is a linear dependence of internal-bias field modified coercive field on frequency.[30]

We found that coercive field broadness ($2E_C$) of BTBCN single layer was 7.2 kV/cm and for BT single layer this value was 6.2 kV/cm. In multilayer systems, if they are in uncoupled state behaving like capacitors in series, normally the coercive field broadness should be between 6.2 and 7.2 kV/cm. This was not the case for graded bilayer and trilayer systems as shown in Table II. The lower coercive field broad-

TABLE II. Magnitude of coercive field broadness ($2E_C$) and internal-bias field for various composite systems.

System	Coercive field broadness, $2E_C$ (kV/cm)	Internal-bias field (kV/cm)
BTBCN single layer	7.2	2.9
BT single layer	6.2	1.0
Bilayer with equal thickness	8.2	2.1
Bilayer with unequal thickness	5.1	1.2
Trilayer	8.8	2.5

ness value found in bilayer with unequal thickness system and higher coercive field broadness values found in bilayer with equal thickness and trilayer systems implies that there was finite interaction across the layers. The polarization mismatch provides direct contribution to internal-bias field which increases from bilayer to trilayer system. In order to achieve domain reversal, the system needs additional energy to overcome barrier due to internal-bias field. Consequently, high coercive field is characteristics of system with high internal-bias field. This explains why the coercive field of trilayer system is highest and it reduces sequentially for bilayer with equal and unequal thickness systems, respectively, as shown in Table II. We can also notice that coercive field for bilayer with unequal thickness system is less than that for BT single layer. This reflects the effect of interface coupling between layers in bilayer with unequal thickness system which enhances domain wall mobility.

The graded trilayer ceramic system was found to exhibit double hysteresis looplike behavior which normally occurs in antiferroelectric materials.[33–37] Prior studies have also found similar behavior and it was attributed to presence of multiple domain states when two factors are simultaneously occurring, (i) the coupling strength (J) between layers is sufficient and (ii), both layers have almost equal polarization values in antiparallel direction ($P_1=-P_2$ or vice versa). The polarization of each layer depends on layer thickness, so in the case of same material the layer thickness should be $L_1 \approx L_2$ (where L_1 and L_2 are thickness of layer 1 and layer 2, respectively) to provide equal polarization in opposite direction. In case of bilayers with equal thickness of same material, when coupling strength is small the overall polarization ($P=P_1+P_2$) is nonzero and the system is in weak ferroelectric phase. As the strength of coupling increases, P approaches zero, and thus the system will exhibit double loop behavior. In the case of graded bilayers consisting of two different materials, the polarizations P_1 and P_2 are variable with coupling strength.[34] The graded trilayer system has two interfaces between BTBCN-BT and BT-BTBCN. Since each couple layers composes of the same materials with same layer thickness, thus it is possible that each couple induces equal polarization but in different direction, which can explain the origin of double hysteresis looplike behavior. Bilayers with equal and unequal thicknesses did not show double hysteresis looplike behavior which could be related to smaller effective interface thickness.

Figure 7(a) shows that the polarization of BTBCN is higher than that of BT. Since polarization is directly proportional to layer thickness,[34] uncoupled state bilayer system with equal thickness should have higher polarization than that of bilayer system with unequal thickness (lower volume fraction of BTBCN). However results show that the polarization of bilayer system with unequal thickness was almost similar to that of bilayer with equal thickness at 50 Hz. Only at lower frequencies of 0.1 Hz, the polarization recorded for bilayer with equal thickness is higher than that of bilayer with unequal thickness (Table I). This again suggests that there is finite coupling occurring in the layered structure which is frequency dependent. This result can be explained by considering the coupling of two layers which establishes new polarization state in each layer due to internal-bias field arising from polarization mismatch.[16] BTBCN possess higher polarization than that of BT, thus smaller thickness of BTBCN in bilayer system with unequal thickness can reach the polarization of BT. By adjusting the thickness of BTBCN we can create a slight polarization mismatch in graded bilayer which will result in weak internal-bias field that will affect the domain reversal. By tailoring the thickness of layers, a higher polarization in graded bilayer system with unequal thickness could be obtained as shown in Fig. 7(b). For the composite having equal thickness of BT and BTBCN, net polarization value in BTBCN layer will be higher as compared to that of BT giving rise to polarization mismatch. As explained in earlier sections, the trilayer specimen possesses higher exchange coupling and increased internal bias due to finite interaction across the layers. Hence, remanent polarization can expected to be lowest in trilayer as compared with single layer and bilayer systems. This was experimentally confirmed in Fig. 7(b).

C. Dynamic scaling relationships

In ferromagnetic materials, the variation in hysteresis area $\langle A \rangle$ with frequency (ω) and magnetic field (h) has been established as power-law scaling relation $A=A_o+h_o^{\alpha}\omega^{\beta}g(\omega/h_o^{\gamma})$ with the exponents α, β, and γ, and A_0 is the loop area at the zero frequency limit. The function g has a nonmonotonic form such that $g(x)\to 0$ as $x\to 0$ or ∞.[38,39] Analogous to ferromagnetics, ferroelectric materials also exhibit hysteresis $\langle A \rangle$ dependence on applied frequency (f) and electric field (E_0). Thus, we used this model to derive hysteresis area as power-law scaling of frequency and electric field as:

$$\langle A \rangle \propto f^m E_0^n, \tag{20}$$

where m and n are exponents that depend on the dimensionality and symmetry of the system. By plotting $\langle A \rangle$ against f at fixed E_0, one obtains the exponent m. The exponent n can be obtained by plotting $\langle A \rangle$ against E_0 at fixed f.[11] This method can be repeated for all the cases studied here to extract the magnitude of exponent m and n. After obtaining f-exponent m and E_0-exponent n, the scaling of hysteresis area $\langle A \rangle$ against frequency f and field amplitude E_0 can be obtained as shown in Figs. 8(a)–8(d). Noticeably, for each case the scaling relations can be divided into two regimes corresponding to subcoercive field and saturated field condition which possess different domain switching mechanisms. The reversible 180° domain switching mechanism is responsible for changes occurring in subcoercive field condition whereas the irreversible non-180° domain switching mechanism dominates in saturated field condition.[40]

In describing the physical meaning of scaling exponents, the f-exponent m refers to how quickly the domain can switch corresponding to frequency f of electric field switching. A higher negative magnitude for exponent m implies longer switching time where the ferroelectric domains cannot follow the applied ac electric field. Several variables may cause the delay in domain switching including charged defects and space charges.[41] The polarization and hysteresis

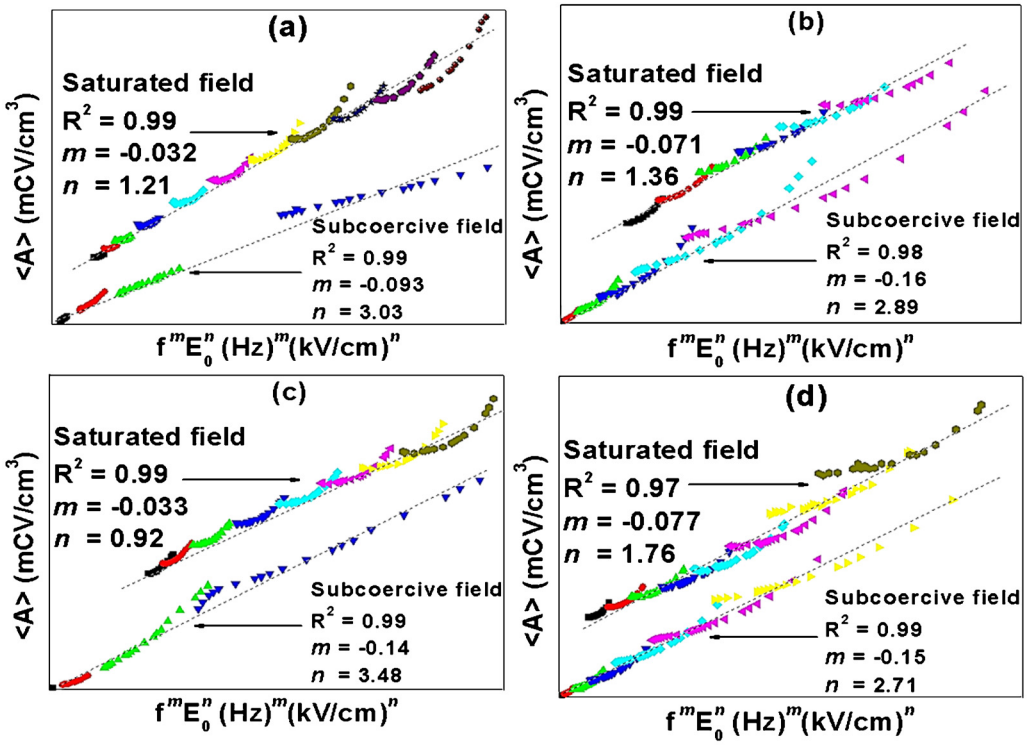

FIG. 8. (Color online) Scaling relations for subcoercive and saturated field conditions (a) BT single layer system, (b) bilayer with equal thickness system, (c) bilayer with unequal thickness system, and (d) trilayer system. Dotted lines indicate linear relations fitted to data in each regime.

area $\langle A \rangle$ decrease rapidly with increase in negative coefficient of m. On the other hand, if exponent m has lower negative coefficient, this implies that the switching time is short. The ferroelectric domains can follow the applied ac electric field, so the polarization and hysteresis area $\langle A \rangle$ decreases slowly. The E_0-exponent n refers to the ease of domain wall motion. The high exponent n value refers to the ability of domain in following the applied electric field direction, so that hysteresis parameters $(\langle A \rangle, P_r, E_C)$ increase sharply with increasing E_0. Conversely, the low exponent n refers to the poor ability of domain switching in following the direction of applied electric field, so hysteresis parameters increase slowly.[11]

Table III shows the power-law scaling exponent m and n for subcoercive and saturated field conditions for all cases. Comparatively, the exponent m of BT single layer system under subcoercive field condition has lower negative value (-0.093) than that of BT bulk ceramic[40]. Generally, domains of material with smaller grain size would respond to switching field slowly than that of material with larger grain size because it possess high density of grain boundaries. However in our case, BT single layer with smaller grain size was found to exhibit lower negative value of exponent m than that of BT bulk ceramic possessing larger grain size. This could be explained by considering exponent m as rate of decrease in domain response with increasing frequency f. Generally, as frequency increases the domain response will be delayed. This effect is further amplified in materials with smaller grain size. Since domain wall velocity is already small, a further increase in frequency does not have much effect. This is why exponent m of BT single layer has lower negative coefficient than that of BT bulk ceramic. In addition, exponent m of BT single layer has the lowest negative value compared with that of graded bilayer and trilayer ceramic systems. This can be related to internal-bias field in this system as discussed earlier. The exponent n in subcoer-

TABLE III. List of exponent m and n in power-law scaling relations for various composite systems.

	Subcoercive field		Saturated field	
System	Exponent m	Exponent n	Exponent m	Exponent n
BT single crystal (previous work[a])	$1.667E_0-2.804$	4.157	−0.195	0.95
BT bulk ceramic (previous work[b])	−0.36	3.64	−0.23	0.87
BT single layer	−0.093	3.03	−0.032	1.21
Bilayer equal thickness	−0.16	2.89	−0.071	1.36
Bilayer unequal thickness	−0.14	3.48	−0.033	0.92
Trilayer	−0.15	2.71	−0.077	1.76

[a]Reference 24.
[b]Reference 40.

cive field condition for BT single layer is smaller than that of BT single crystal and BT bulk ceramic. Basically, domain switching mechanism in subcoercive field condition is related to reversible 180° domain switching or amount of domain volume which is proportional to grain size. Consequently, BT single layer possessing smaller grain size should have smaller exponent n value. Surprisingly, exponent n of BT single layer was not the highest when compared with bilayer and trilayer systems. The highest value of exponent n was found to be for graded bilayer with unequal thickness as listed in Table III. This could be caused by enhancement in domain wall mobility occurring from coupling between layers. The exponent n of trilayer composite was lowest owing to its high internal bias which pins the domain wall motion.

In saturated field condition, the exponent m of BT single layer had lower negative value compared to both BT single crystal and BT bulk ceramic. Upon comparison with bilayer and trilayer composites, we can find that exponent m of BT single layer had distinctively lower negative value than that of bilayer with equal thickness and trilayer systems but similar to that of bilayer with unequal thickness. This phenomenon can be attributed to strength of internal-bias field. BT single layer and bilayer with unequal thickness systems have weak and similar internal-bias field value as listed in Table II, thus exponent m has lower negative value. The internal-bias field for bilayer with equal thickness and trilayer composites is quite large so exponent m has higher negative coefficient. From Table III, we can see that the exponent n for BT single layer was higher than that for BT single crystal and bulk ceramic. Since hysteresis behavior near saturated polarization does not change much, BT single layer may have distinct exponent n than that in BT single crystal and bulk ceramics which were measured below the saturated field condition. Comparing bilayer and trilayer composites, the exponent n was highest for trilayer while the smallest for bilayer with unequal thickness. It is very interesting that exponent n values of both systems invert from subcoercive field condition. The trilayer composite with lowest exponent n under subcoercive field condition possess the highest value under saturated field condition, while the bilayer with unequal thickness has the highest n coefficient under subcoercive field condition but it changes to lowest one under saturated field condition. This may be related to the magnitude of internal-bias field which is highest for trilayer as shown in Table II. Thus, these composites provide a wide range of tuning capability of ferroelectric polarization, coercive field, and hysteresis area, by varying the grading and number of layers.

IV. CONCLUSION

In summary, graded bilayer and trilayer bulk composite of BT and BTBCN were synthesized with different thickness of individual layer while keeping the same overall effective thickness. TEM and SEM images depicted a sharp interface with needle shape domains across the interface. The domain size was found to be larger on BT side as compared to that on BTBCN side. Temperature dependence of dielectric response for all composite systems was found to exhibit shifting in Curie peak with respect to each constituent material due to coupling between layers. Polarization mismatch between uncoupled BT and BTBCN resulted in internal electric field in composite specimen which produces new polarization states in each layer by perturbing free energy of the composite specimen. Further, the differences in grain size, tetragonality, and domain mobility of each layer also perturbs the electrical response in coupled layered composites. The dynamic hysteresis behavior and power-law scaling relations of BT single layer, bilayer with equal and unequal thickness, and trilayer ceramic systems were derived. All cases exhibited similar trends where hysteresis area $\langle A \rangle$, remnant polarization (P_r), and coercive field (E_C) was found to decrease with increasing frequency due to delayed response. But, the magnitude of these hysteresis parameters was found to increase with increase in applied electric field due to enlargement of electrical driving force. Graded trilayer system was found to possess the strongest internal-bias field while graded bilayer with unequal thickness system had the lowest magnitude. The trilayer composite was found to exhibit the double hysteresis loop due to polarization mismatch between layers.

ACKNOWLEDGMENTS

The authors gratefully acknowledge financial support from DMR, National Science Foundation (Materials World Network Program); Office of Basic Energy Sciences, Department of Energy (Contract No. DE-FG02–07ER46480); and the Fundamental R&D Program for Core Technology of Materials funded by the Ministry of Knowledge Economy, Republic of Korea. The authors would also like to thank NCFL, VT for their help in characterization.

[1]H.-T. Lue and C.-J. Wu, IEEE Trans. Electron Devices **49**, 1790 (2002).
[2]S. L. Miller and P. J. McWhorter, J. Appl. Phys. **72**, 5999 (1992).
[3]M. Ullmann, H. Goebel, H. Hoenigschmid, and T. Hander, IEICE Trans. Electron. **83**, 1324 (2000).
[4]K. H. Kim, J. P. Han, S. W. Jung, and T. P. Ma, Electron Device Lett., IEEE **23**, 82 (2002).
[5]J. Wu, J. Zhu, D. Xiao, and J. Zhu, Appl. Phys. Lett. **91**, 212905 (2007).
[6]I. Essaoudi, A. Ainane, M. Saber, and J. J. de Miguel, Phys. Status Solidi B **244**, 3398 (2007).
[7]Y.-Z. Wu, D.-L. Yao, and Z.-Y. Li, J. Appl. Phys. **91**, 1482 (2002).
[8]J. F. Scott, Ferroelectr. Rev. **21**, 1 (1998).
[9]K. Uchino, *Ferroelectric Devices*, 2nd ed. (CRC/Taylor & Francis Group, FL, 2010).
[10]R. Waser, U. Böttger, and M. Grossmann, in *Ferroelectric Random Access Memories*, edited by H. Ishiwara, M. Okuyama, and Y. Arimoto (Springer-Verlag, Berlin, 2004).
[11]N. Wongdamnern, N. Triamnak, M. Unruan, K. Kanchianga, A. Ngamjarurojana, S. Ananta, Y. Laosiritaworn, and R. Yimnirun, Phys. Lett. A **374**, 391 (2010).
[12]K. Uchino, E. Sadanaga, and T. Hirose, J. Am. Ceram. Soc. **72**, 1555 (1989).
[13]W. Cao and C. A. Randall, J. Phys. Chem. Solids **57**, 1499 (1996).
[14]C.-W. Ahn, D. Maurya, C.-S. Park, S. Nahm, and S. Priya, J. Appl. Phys. **105**, 114108 (2009).
[15]K. Chi Kao, *Dielectric Phenomena in Solids* (Elsevier Academic, San Diego, 2004).
[16]C. Wood, and D. Jena, *Polarization Effects in Semiconductors From Ab Initio Theory to Device Applications* (Springer, New York, 2008).
[17]R. Kretschmer and K. Binder, Phys. Rev. B **20**, 1065 (1979).
[18]B. Strukov and A. Levanyuk, *Ferroelectric Phenomena in Crystals* (Spring-Verlag, Berlin, 1998).
[19]N. Wongdamnern, N. Triamnak, A. Ngamjarurojana, S. Ananta, Y. Lao-

siritaworn, and R. Yimnirun, Ferroelectrics **384**, 1 (2009).
[20]D. Maurya, C.-W. Ahn, S. Zhang, and S. Priya, J. Am. Ceram. Soc. **93**, 1225 (2010).
[21]E. Fatuzzo and W. J. Merz, in *Ferroelectricity*, 1st ed., edited by E. P. Wohlfarth (Wiley, New York, 1967), Vol. 7, Chap. 1, p. 5.
[22]W. J. Merz, Phys. Rev. **95**, 690 (1954).
[23]A. Picinin, M. H. Lente, J. A. Eiras, and J. P. Rino, Phys. Rev. B **69**, 064117 (2004).
[24]N. Wongdamnern, A. Ngamjarurojana, Y. Laosiritaworn, S. Ananta, and R. Yimnirun, J. Appl. Phys. **105**, 044109 (2009).
[25]K. Okazaki and K. Sakata, Electrotechnical Journal of Japan **7**, 13 (1962).
[26]R. E. Cohen, J. Phys. Chem. Solids **61**, 139 (2000).
[27]M. H. Lente and J. A. Eiras, J. Phys.: Condens. Matter **12**, 5939 (2000).
[28]M. H. Lente and J. A. Eiras, J. Appl. Phys. **89**, 5093 (2001).
[29]S. Takahashi, Ferroelectrics **41**, 143 (1982).
[30]A. S. Sidorkin, L. P. Nesterenko, S. V. Ryabtsev, and A. A. Sidorkin, Phys. Solid State **51**, 1348 (2009).
[31]S. Takahashi, Jpn. J. Appl. Phys. **20**, 95 (1981).
[32]A. S. Sidorkin, *Domain Structure in Ferroelectrics and Related Materials* (Cambridge International Science Publishing, Cambridge, UK, 2006).
[33]L. H. Ong, J. Osman, and D. R. Tilley, Phys. Rev. B **65**, 134108 (2002).
[34]Y. Q. Ma, J. Shen, and X. H. Xu, Solid State Commun. **114**, 461 (2000).
[35]K. H. Chew, L. H. Ong, J. Osman, and D. R. Tilley, Appl. Phys. Lett. **77**, 2755 (2000).
[36]K. H. Chew, Y. Ishibashi, F. G. Shin, and H. L. W. Chan, J. Phys. Soc. Jpn. **72**, 2364 (2003).
[37]N. Wongdamnern, J. Tangsritragul, A. Ngamjarurojana, S. Ananta, Y. Laosiritaworn, and R. Yimnirun, Mater. Chem. Phys. **124**, 281 (2010).
[38]M. Acharyya, Phys. Rev. E **56**, 1234 (1997).
[39]B. K. Chakrabarti and M. Acharyya, Rev. Mod. Phys. **71**, 847 (1999).
[40]N. Wongdamnern, A. Ngamjarurojana, S. Ananta, Y. Laosiritaworn, and R. Yimnirun, Key Eng. Mater. **421–422**, 399 (2010).
[41]R. Yimnirun, R. Wongmaneerung, S. Wongsaenmai, A. Ngamjarurojana, S. Ananta, and Y. Laosiritaworn, Appl. Phys. Lett. **90**, 112908 (2007).